Flora 253 (2019) 87–97

Contents lists available at ScienceDirect

Flora

journal homepage: www.elsevier.com/locate/flora

Morphological and anatomical characteristics and temporal pattern of initial growth in *Astrocaryum acaule* Mart

Marcos Melo Corrêa[a,*], Maria Gracimar Pacheco de Araújo[b], Maria Silvia de Mendonça[c]

[a] Instituto Nacional de Pesquisas da Amazônia – INPA, Programa de Pós-Graduação em Botânica, Manaus, Amazonas, Brazil
[b] Laboratório de Anatomia Vegetal, Departamento de Biologia, Instituto de Ciências Biológicas - ICB I, Campus Setor Sul, Universidade Federal do Amazonas, Av. Rodrigo Octávio Jordão Ramos, 3000, Manaus, Amazonas, Brazil, CNPq Productivity Scholarship
[c] Laboratório de Botânica Agroflorestal, Faculdade de Ciências Agrárias – FCA, Campus Setor Sul, Universidade Federal do Amazonas, Av. Rodrigo Octávio Jordão Ramos, 3000, Manaus, Amazonas, Brazil, CNPq Productivity Scholarship

ARTICLE INFO

Edited by Alessio Papini

Keywords:
Amazon
Germination
Palm
Seedling
Tucumã-í

ABSTRACT

Astrocaryum acaule Mart. is a palm with underground stem, common in lowland forests, known in Brazil as tucumã-í. The objective of this work was to perform the description and characterization of seeds and of the seedling emergence process, revealing morphological and anatomical patterns of *A. acaule*. Seedlings were obtained by sowing in vermiculite. The seed is spherical, with variations in shape and size according to the number of seeds in the fruit. Germination is adjacent, with formation of a coleoptile above the cotyledonary sheath. The germinative bud is emitted within between 30 and 130 days. The proximal and distal regions differentiate with growth, forming the seedling and the haustorium that transfers reserves through the reduced apocole. The initial root system differs in the hypocotyl-radicle region, below the insertion of leaf primordia, forming a lateral root and a late primary root. The first eophyll is expanded 120 days after the protrusion of the germinative button, with aculeate petiole, amphistomatic leaf blade, papillose epidermis, homogeneous mesophyll, and vascular system covered by fibers. Morphoanatomical characters reported in this study increase our knowledge about Amazonian palms and on organogenesis in their early stages of growth.

1. Introduction

Palms (Arecaceae) are one of the most characteristic and abundant groups of tropical rainforest plants, and display a great variety of reproductive strategies (Rojas-Robles and Stiles, 2009). In addition to being a diverse group within the Amazon rainforest, Arecaceae are ecologically important for the maintenance of vertebrate animal biomass, especially during seasons of fruit scarcity (Cintra et al., 2005).

The anatomy of seedling development is little studied, but deserves greater attention, since the early developmental period of a plant constitutes a critical phase in the life cycle of many species, as seedlings depend on the spatio-temporal congruence of a suite of environmental factors for successful establishment (Gurski, 2007). Anatomical studies can help establish an understanding of how physiological and structural processes interact with environmental conditions to determine within-habitat distributions, thus providing important key information for species natural histories (Mourão et al., 2002), which is essential for effective conservation. An applied knowledge of seed and seedling morphology allows structures to be identified and interpreted in a functional context. This then allows the most appropriate germination tests and sample quality monitoring to be implemented. In addition, it can help seedling production methods for a variety of purposes, including reforestation, as well as ornamental large-scale production (Groth and Liberal, 1988).

Native palms adjust more swiftly to agroforestry systems than do introduced species, since they are already adapted to local forest conditions (Queiroz and Bianco, 2009). Consequently, information on the morphological aspects of germination can also be used when domesticating potentially economically-useful native species (Oliveira et al., 2010). In the Amazonian context, the current study of *Astrocaryum acaule* Mart. represents an important contribution to general knowledge of the family Arecaceae, as well as to the greater understanding the Amazonian biota, since not only is it a highly characteristic species of the region, with economic potential, but is still poorly-known scientifically.

Astrocaryum acaule is a palm with an underground stem, and is common in lowland Amazonian forests. The species is placed in the subfamily Arecoideae, tribe Cocoseae, subtribe Bactridinae (Uhl and

* Corresponding author.
E-mail addresses: marcos.melo.correa@outlook.com (M.M. Corrêa), mariagalpacheco@gmail.com (M.G.P.d. Araújo), msilvia@ufam.edu.br (M.S.d. Mendonça).

https://doi.org/10.1016/j.flora.2019.03.005
Received 13 December 2018; Received in revised form 8 March 2019; Accepted 11 March 2019
Available online 16 March 2019
0367-2530/

Dransfield, 1987; Lorenzi, 2010). According to Henderson (1995), *A. acaule* is commonly known in Brazil as *tucumã-í* or *tucumaí*, in Colombia as *espina, cocorito, tucum*, *mataukari*, and as *corozo* in Venezuela (Stauffer, 2000). Tucumã-í is a common palm of flooded forests along the Rio Negro and many of its tributaries, and also occurs in sandy areas along the banks of clear-water rivers, such as the Tapajós. It is covered by black spines, typical of the genus, that leave scars upon detachment, especially on the petioles (Henderson, 1995; Dransfield et al., 2008). The leaves can reach more than 5 m in length, and the young petioles have a distinctive reddish-brown color.

The objective of the current study was to describe the initial seedling growth process of *A. acaule* in terms of morphology and anatomy, as well as recording the temporal and ontogenetic patterns of germination, and compare the results with the associated nomenclature and available literature on the subject.

2. Material and methods

The study was carried out using seedlings grown from seeds obtained from fruits collected in the Tupé Sustainable Development Reserve, Amazonas State, Brazil. The reserve is located on the left bank of the Rio Negro, some 25 km west of Manaus city center. It has an average altitude of 20 m above sea level, a total area of 11,973 ha, and a perimeter of 47,056 m (Santos-Silva, 2008).

Anatomical analyzes were performed in the Agroforestry Laboratory of the Agricultural Sciences Faculty (LABAF-FCA), Federal University of Amazonas (UFAM). The epicarp and the mesocarp were removed with a domestic knife from the collected fruits (Fig. 1A). Next, after drying at room temperature for 10 days, the endocarp of each fruit was broken with a bench vise, and the seed extracted (Fig. 1B). Drying the fruit facilitates the detachment of the seed from the endocarp interior (Ferreira and Gentil, 2006). The resulting 300 seeds were soaked in distilled water to accelerate the germination process, then planted in perforated plastic trays containing vermiculite as substrate. Of these, 70 were analyzed morphometrically with digital calipers, and weight measured with a precision balance.

Once germinated, seedlings were monitored for classification into ontogenetic stages, and records tabulated using Microsoft Excel 2016 software. Timelines for the production of structures of interest were based on records from 100 seedlings.

Development was tracked from the appearance of initial germinative bud to the expansion of the first eophyll (true leaf). Samples for anatomical analysis were fixed in FAA70 (Formalin –Alcohol – Acetic Acid), dehydrated in an ethanolic series (Berlin and Miksche, 1976 apud Kraus and Arduin, 1997), placed in 2-hydroxyethyl methacrylate (Leica Historesin®, prepared according to the manufacturer's instructions), sectioned longitudinally and transversely in a rotating microtome with slices of 5 to 7 µm thickness. For the stages from the first cataphyll (scale leaf) onwards, the slices were made preferentially at the base of the embryonic axis. Sections were stained with 0.05% toluidine blue (O'Brien et al., 1964), and slides mounted in water. As an auxiliary method, fresh slices were prepared with a tabletop microtome, clarified with sodium hypochlorite, stained with 1% Astra blue and safranin 1% (Safrablau 9:1) (Bukatsch, 1972) in aqueous solution, and slides mounted in glycerinated gelatin (Kaiser, 1980 apud Kraus and Arduin, 1997).

For seedlings with the first eophyll expanded, the primary root, petiole and emergent tip of the eophyll were analyzed using cross-sections obtained from the median region of each structure. This was done with a table microtome, clarified with sodium hypochlorite 50%, stained with Astra blue 1% and safranin 1% (safrablau 9:1) (Bukatsch, 1972), and the resultant semipermanent slides mounted in glycerinated gelatin. To obtain samples of the epidermis, 1 cm^2 slices were immersed in a 30% hydrogen peroxide + acetic acid solution (1:1) (Franklin, 1945), stained with safranin and mounted in glycerinated gelatin.

Parameters for description followed Queiroz (1986); Tomlinson (1990); Henderson (1995), Henderson (2006) and Tillich (2007). Photographs were taken with a Panasonic Lumix DMC-LS80 digital camera, and photomicrographs obtained using a Canon PC1252 digital camera coupled to a Zeiss Primo Star MicroImaging 37081 photomicroscope.

3. Results

Seeds of *A. acaule* are generally spherical, with a mean length of 14.11 mm and diameter of 13.01 mm (n = 70; SD = 1.46 and 1.04, respectively). Average fresh mass was 1.38 g (n = 70; SD = 0.29). The seed is weakly attached to the enveloping endocarp. The seed surface display two depressions, where ovules were located prior to fertilization. The integument is dark brown streaked with gray. The endosperm

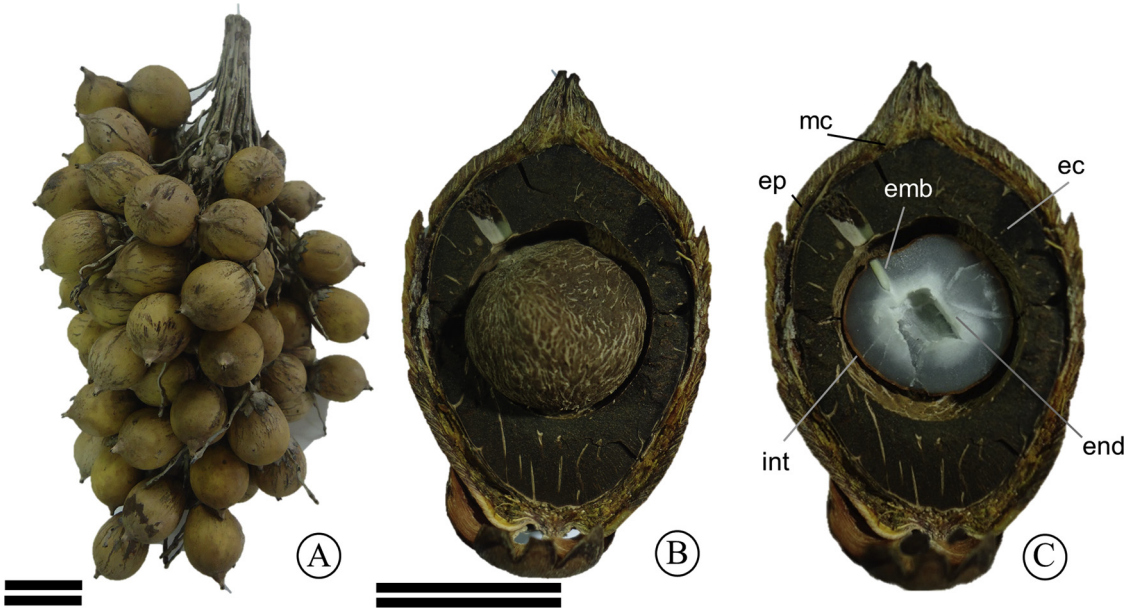

Fig. 1. Infructescence and fruits in *Astrocaryum acaule* Mart. A) Infructescence; B) Detail of fruit, showing the position of the seed; C) Detail of fruit, showing the position of the embryo in the seed. ep: epicarp, ec: endocarp, emb: embryo: end: endosperm, int: integument, mc: mesocarp. Scale: A = 4 cm, B - C = 2 cm.

Table 1
Mean measurements for *Astrocaryum acaule* Mart. seeds in fruits with one and two seeds (n = 70).

	1 seed			2 seeds			
	length	diameter	mass	length	width	depth	mass
Mean	14.11	13.04	1.39	12.88	12.12	7.34	0.78
Minimum	9.25	9.81	0.34	10.34	10.16	4.93	0.34
Maximum	17.56	14.85	1.93	15.69	14.40	8.55	1.14
Standard deviation (±)	1.46	1.04	0.29	1,89	1.44	1.29	0.27

is stiff and whitish in the mature seed. The embryo is white to greenish, and lies in the apical region, near the micropyle, diagonally to seed axis (Fig. 1C). In the endocarp with two seeds (n = 6; 8,5% of the seeds), one of the faces of each seed was flattened, and seeds had a mean length of 12.88 mm, width of 12.12 mm, and depth of 7.34 mm (SD = 1.89, 1.43, and 1.29, respectively) (Table 1). The species showed adjacent germination (the seedling develops near the seed), with the formation of a coleoptile above the cotyledon sheath (Fig. 2).

3.1. Germinative bud formation

Germination was uneven (staggered), with the formation of the germinative bud varying between 30 and 130 days. The germinative bud was about 2 mm long, whitish, cylindrical, and straight on emergence (Fig. 2A), with a constriction between the haustorium and the point of cotyledonary sheath swelling. Overall, this region tended to swell some 10 days after bud development, when it became greenish and acquired a swollen triangular shape, a result of embryonic axis elongation within the cotyledonary sheath (Fig. 4).

At this developmental stage, the distal region has yet to expand in volume beyond the cavity occupied by the embryo. Despite the formation of a rigid structure rich in phenolic compounds (Fig. 2B), the radicle does not penetrate the cotyledonary sheath tissues and, in some individuals, this stage may be postponed until the first eophyll emerges.

3.2. First cataphyll protrusion

The first cataphyll, also known as the first sheath, emerged about 15 days after the protrusion of the germinative bud. It is whitish in color, conical in shape, and usually lacks surface aculei, though these may appear later (Fig. 2C). At this stage, the first root reaches an average length of 1.4 cm, and the first cataphyll is 0.6–1 cm long.

The formation of a transitional region between the stem meristem and the hypocotyl-radicle region becomes evident. This region is composed of ground meristem and procambial strands. These vascular traces are oriented horizontally to the substrate, giving rise to the radicle that will form the first root system. At this point, the aerial part differentiates into cataphylls and the first leaves.

3.3. Second cataphyll protrusion

From the second cataphyll expansion stage (about 20 days after the germinative bud formation), secondary roots may emerge from the primary root system. The second cataphyll is conical, whitish to greenish when above the substrate, and may be aculeate (Fig. 2D), reaching up to 2.0 cm in length.

3.4. First eophyll protrusion and expansion

The first eophyll protruded about 69 days after the germinative bud, and expanded at around 120 days, reaching 8.0 x 1.0 cm. The structure is initially highly plicate, only becoming bifid as it expands (Fig. 2E). At the expanded eophyll seedling stage, the first cataphyll reached the average length of 1.2 cm, and the second, 2.4 cm, while the primary root attained 30 cm, with lateral roots branching from it. Until the expansion stage of the first eophylls, the stem region nodes are inconspicuous. This reflects in the anatomical structure of the hypocotyl region, which contains large numbers of meristematic cells and procambial traces (Figs. 4I, 5 C). Haustorium growth, which occurs as result of endosperm reserve consumption, can be observed throughout the developmental process (Fig. 2). Endosperm reserves have been depleted at the moment of first eophyll expansion, but the haustorium has not yet reached the total seed volume.

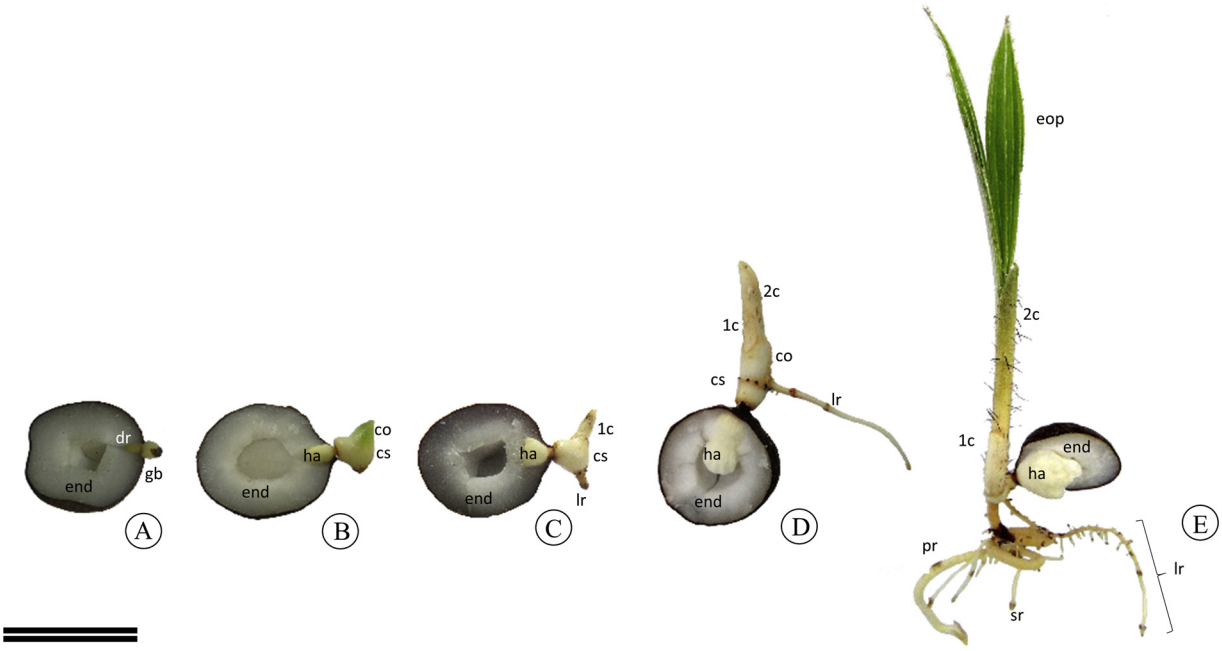

Fig. 2. Stages in the initial growth of *Astrocaryum acaule* Mart. illustrating the development of the haustorium. A) germinative bud; B) swollen bud; C) appearance of the first cataphyll; D) appearance of the second cataphyll; E) appearance of the first eophyll. 1c: first cataphyll, 2c: second cataphyll, ar: adventitious root, dr: distal region, end: endosperm, eop: eophyll, gb: germinative bud, ha: haustorium, lr: lateral root, pr: primary root. Scale: 2 cm.

Table 2
Time in days for the emission of the germinative bud and between the developmental stages of *Astrocaryum acaule* Mart. seedlings.

	germinative bud	swollen bud	1st. cataphyll	2nd. cataphyll	eophyll appearance	eophyll expansion
Mean	112.8	7.7	15.2	20.0	26.2	51.6
Minimum	14	3	8	5	10	28
Maximum	250	18	27	41	54	71
Standard deviation (±)	73.8	4.8	5.6	11.0	14.8	17.0

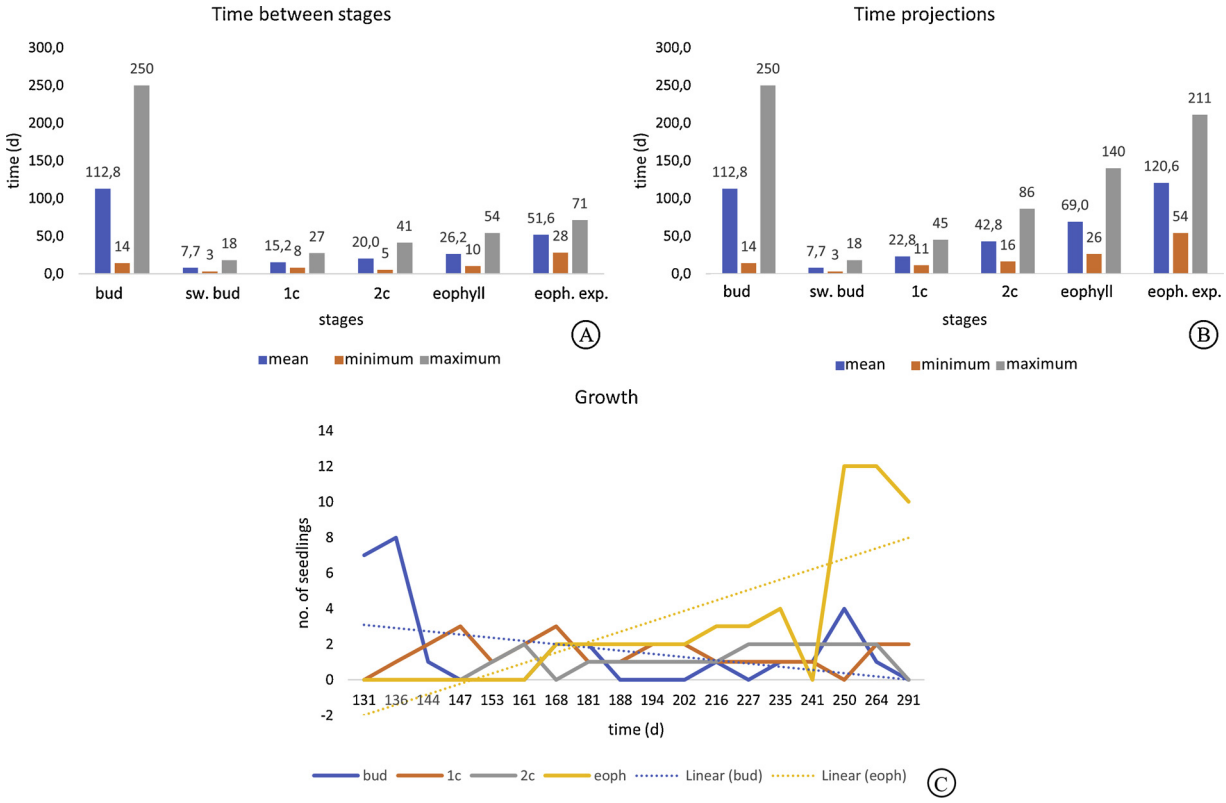

Fig. 3. Time of the developmental stages of seedlings of *Astrocaryum acaule* Mart.
A) Time for germinative bud appearance, and lag between *Astrocaryum acaule* Mart. developmental stages; B) projections based on the sum of the mean, minimum and maximum time between each seedling stage; C) number of records in a sample of 100 individuals showing established stages. 1c: first cataphyll, 2c: second cataphyll, eoph.: eophyll, eoph. exp.: eophyll expansion, sw. bud: swollen bud.

Germination time mean was of 112.8 days (Table 2), but large variation (minimum 14, maximum 250), characteristic of a staggered germination strategy was recorded. The time between stages was also variable, with eophyll expanding up to 71 days after appearance (Table 2, Fig. 3A). By adding up interstage intervals, we arrive at mean developmental stage duration, with eophylls expanding about 120.6 days after the protrusion of the germinative bud (Fig. 3B).

For 100 of the seeds in the sample, there was a trend of individuals to produce a germinative bud between 130–150 days after sowing. Between 250–290 days, most seedlings were in the eophyll expansion stage (Fig. 3C), and high seedling mortality (69%) was recorded.

3.5. Anatomy

In longitudinal view, the *A. acaule* germinative bud is cylindrical, with the distal region slightly flattened, resembling the shape of the embryo (Fig. 4A). The embryonic axis is proximal (Fig. 4B), and indicated by a cleft in the cotyledonary sheath located near the apex of the leaf primordia that will form the cataphylls, and appearing before eophylls (Fig. 4C). Distally, a set of meristematic tissues that eventually differentiates into the haustorium and the apocole can be seen (Fig. 4D), though these are reduced in *A. acaule* as result of the adjacent type of initial growth.

Oliveira et al., 2010;The proximal region begins to swell with the growth of the plumule and the elongation of the radicle (Fig. 4E; 5 B, E, G), which eventually breaches the tissues located in the cotyledonary cleft region (Fig. 4C). The coleoptile is formed by the extending cotyledonary sheath towards the aerial section, with many vascular bundles projecting from the sheath base (Fig. 4E, 6 A - G). The appearance of the radicle may be delayed until eophyll protrusion, although a root cap containing numerous idioblasts is already being formed at the stage of first cataphyll appearance (Fig. 4F, 5 B).

3.6. Root system formation

The seedling is nourished and physically oriented with the aid of a complex root system. The radicle extends relatively late, either when the second cataphyll emerges or when the first eophyll expands (Fig. 2E). This system begins to differentiate with the emergence of the first cataphyll (Fig. 4). The radicle elongates slightly, followed by an accumulation of idioblasts containing phenolic compounds in its apical region, forming a cap that will facilitate root penetration into the substrate.

In cross-section of the cotyledonary sheath at the first cataphyll

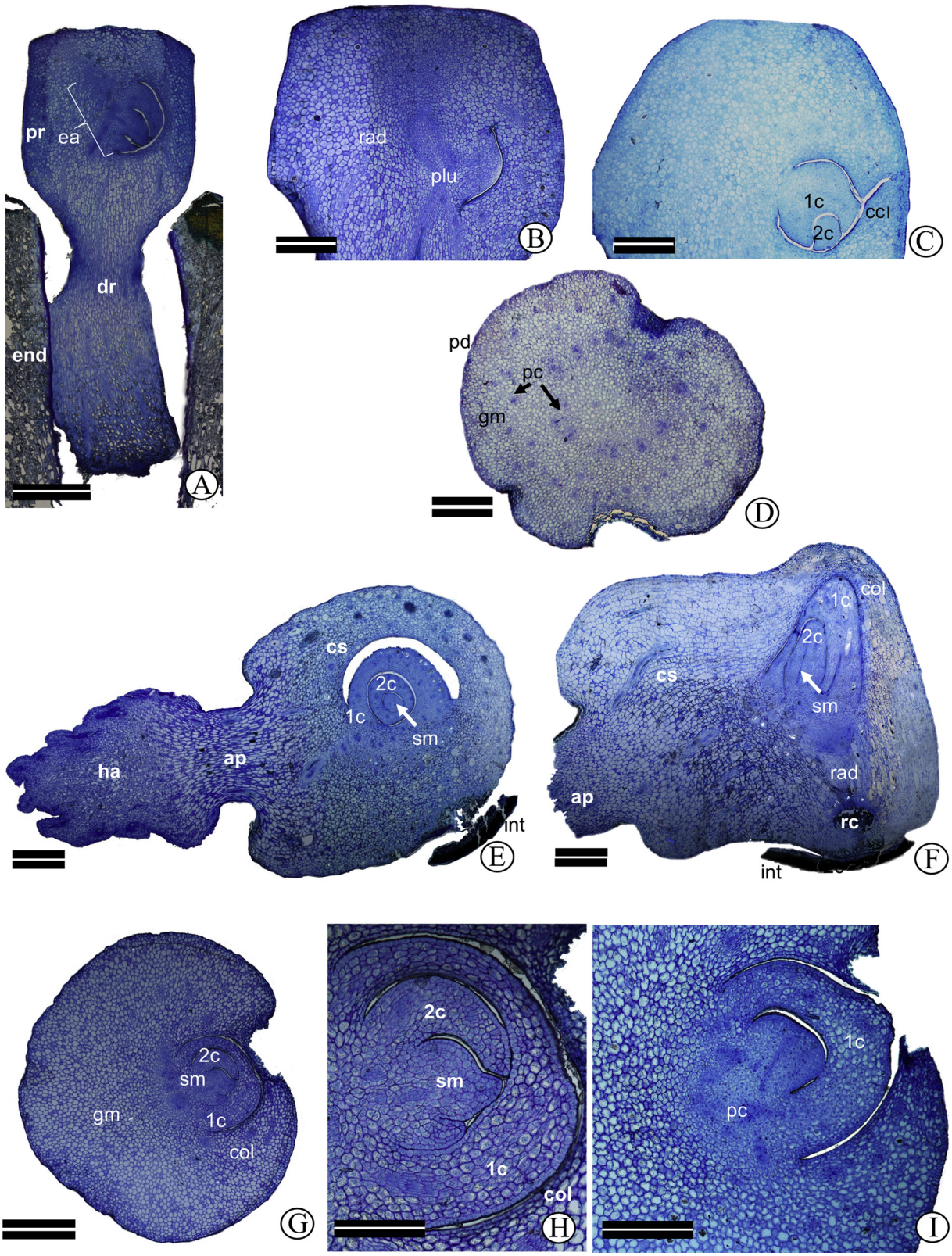

Fig. 4. Germinative bud stage of *Astrocaryum acaule* Mart. A) Longitudinal section of the germinative bud in the seed, showing proximal and distal regions; B) detail of the orientation of the embryonic axis in the proximal region; C) location of the cotyledonary cleft at the plumule apex; D) cross-section of the distal region, corresponding to the apocole region; E) longitudinal section of the bud in the swelling stages; F) longitudinal section of the bud close to the appearance of the first cataphyll; G) bud cross-section in the region of cotyledon sheath rupture; H) detail of G with location of leaf primordia and apical meristem; I) bud cross section in region of cataphyll insertion. 1c: first cataphyll, 2c: second cataphyll, ap: apocole, ccl: cotyledonary cleft, col: coleoptile, cs: cotyledonary sheath, dr: distal region, ea: embryonic axis, end: endosperm, gm: ground meristem, ha: haustorium, int: integument, pc: procambium, pd: protodermis, plu: plumule, pr: proximal region, rad: radicle, rc: root cap, sm: shoot meristem. Scale: A = 500 μm, B - D = 250 μm, E - F = 500 μm, G = 250 μm, H - I = 100 μm.

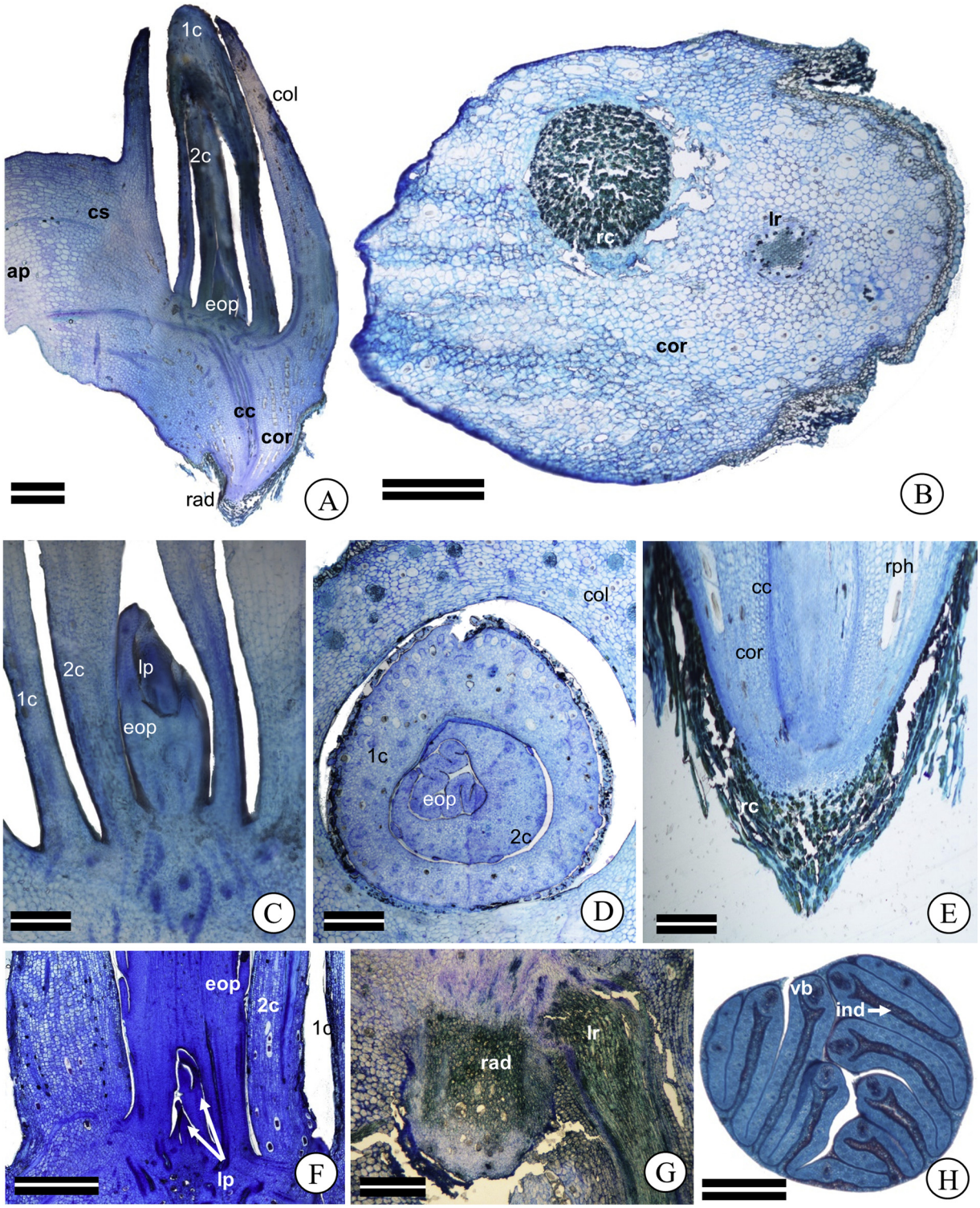

Fig. 5. First cataphyll stage (A–E) and second cataphyll stage (F–H) of *Astrocaryum acaule* Mart. A) Longitudinal section of cotyledonary sheath, showing cataphyll bases, the first eophyll and the radicle; B) detail of root emergence region; C) detail of the cataphyll and leaf primordia initiation region; D) cross section of cataphylls showing location of first eophyll still in development; E) terminal region of the radicle; F) detail of development region for cataphylls and foliar primordia; G) detail of root initiation region; H) first eophyll at plicate stage. 1c: first cataphyll, 2c: second cataphyll, ap: apocole, cc: central cylinder, cor: cortex, col: coleoptile, cs: cotyledonary sheath, eop: eophyll, ind: indument, lr: lateral root, lp: leaf primordium, rad: radicle, rc: root cap, rph: raphid, vb: vascular bundle. Arrows indicate vascular bundles in the coleoptile. Scale: 500 μm.

emergence stage, the procambial vessels are visible from below the point of leaf insertion (Fig. 6A) down to the radicle (Fig. 6B - F), where vessel bundles form a circular structure, surrounded by raphid-containing idioblasts. Idioblasts with phenolic compounds are abundant, particularly in the root cap and its vicinity (Fig. 6G - I). Lateral root differentiation begins on the peripheral area of radicle initiation. As it develops, the root penetrates the tissues of the cotyledonary sheath prior to the emergence of the radicle, forming an angle of 45° to 60°

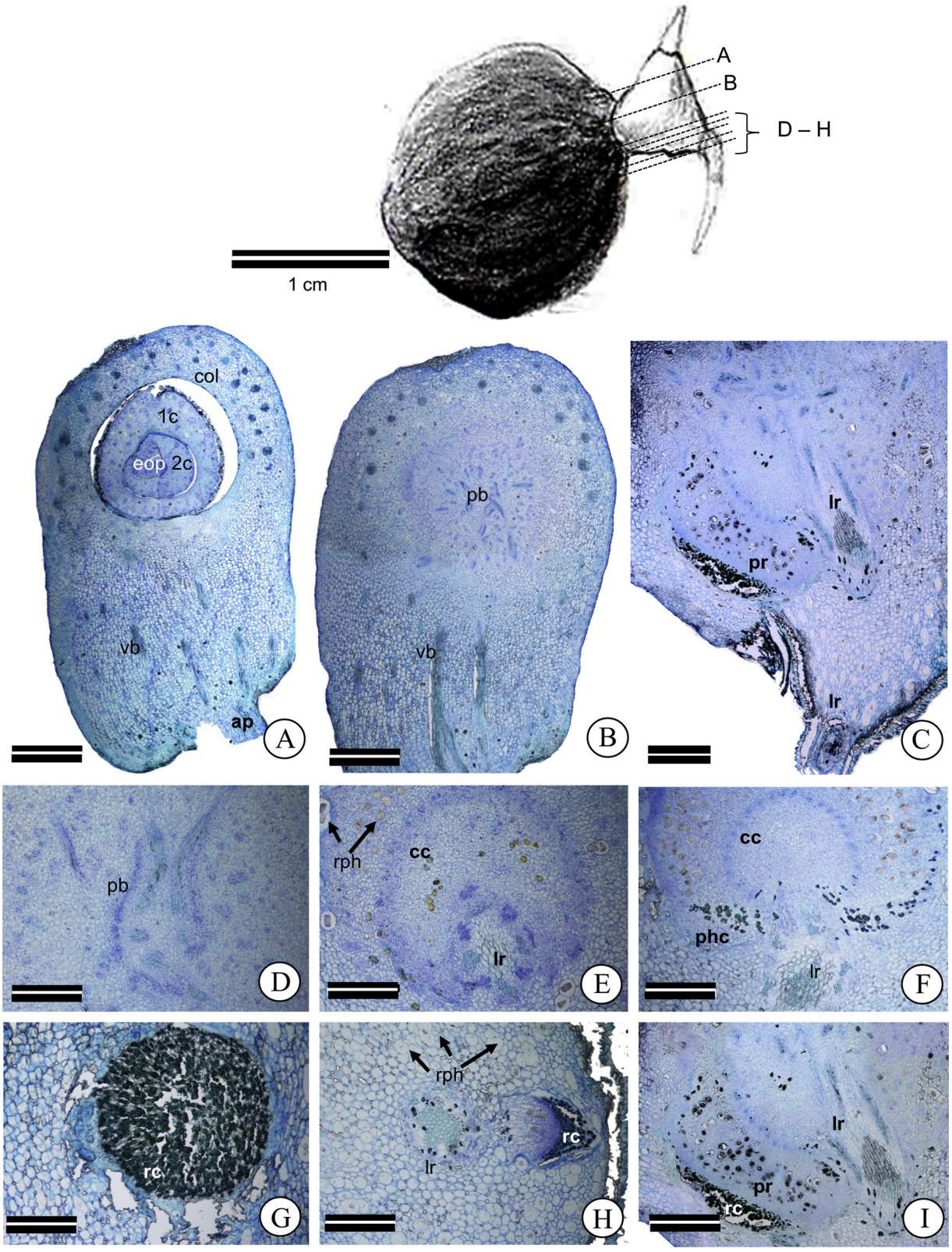

Fig. 6. Sections of the *Astrocaryum acaule* Mart. cotyledonary sheath showing the arrangement of the vascular bundles from the region of foliar primordia insertion to the apex of the radicle during the first cataphyll stage. A) Location of cataphylls, with the first eophyll still in development; B) base of the foliar primordium insertion, showing rich procambial vascularization; C) longitudinal view of the emergence zone first lateral root and primary root; D) organization of the radicle vascular system; E–F) differentiation of the first lateral root at the periphery of the central cylinder; G) radicle apex; H) radicle apex region showing lateral root penetrating cotyledonary sheath tissue; I) longitudinal view of root emergence prior to lateral root curvature. 1c: first cataphyll, 2c: second cataphyll, ap: apocole, cc: central cylinder, col: coleoptile, eop: eophyll, lr: lateral root, pb: procambial bands, phc: phenolic compounds, pr: primary root, rc: root cap, rph: raphids, vb: vascular bundles. Scale: A - C, I = 500 µm, D - H = 200 µm.

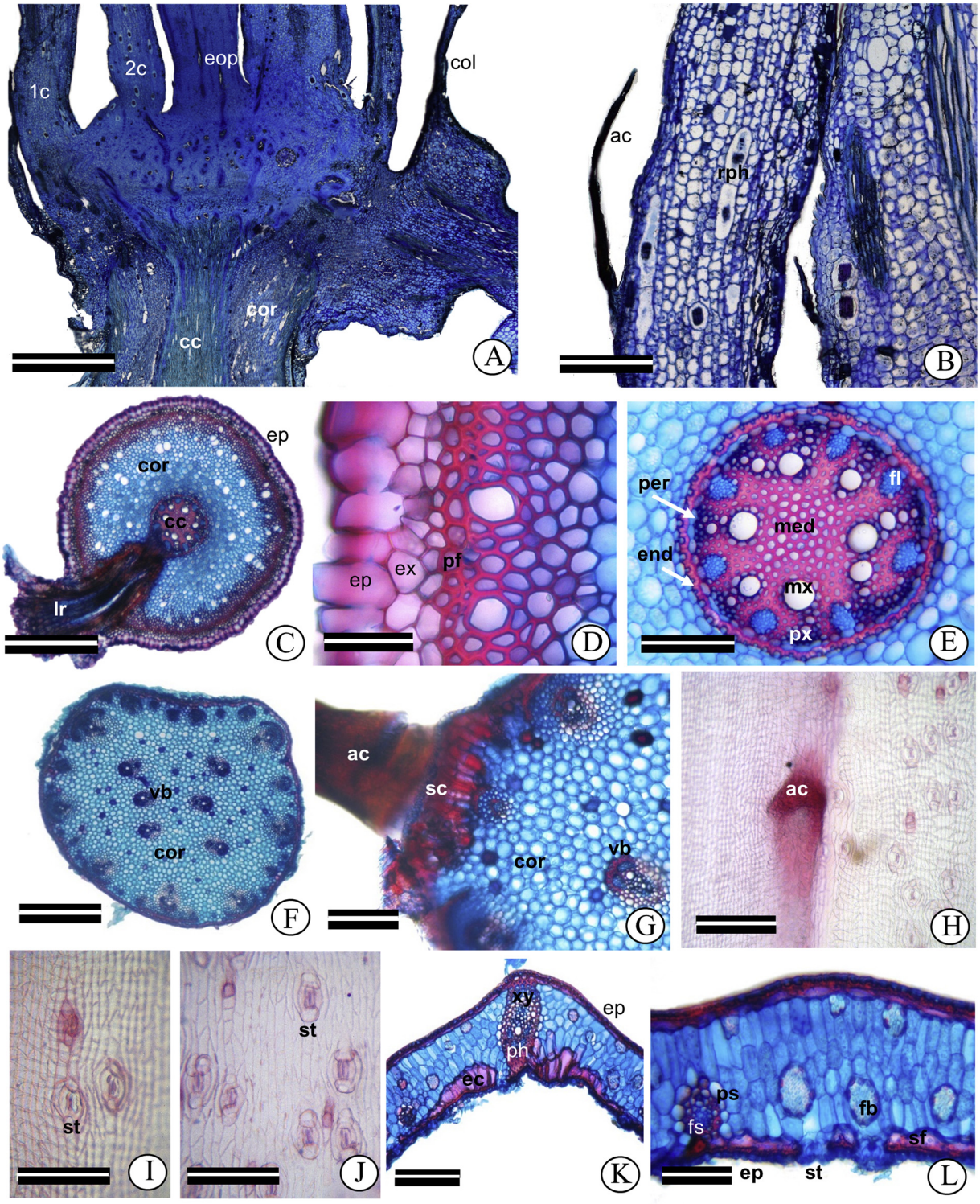

Fig. 7. *Astrocaryum acaule* Mart. expanded eophyll stage A) Cross section showing the arrangement of cataphylls, base of the eophylls and the primary root; B) detail of developing aculei and of raphids in second cataphyll parenchyma; C) Development of lateral root from primary root; D) detail of primary root epidermis; E) detail primary root vascular system; F) cross section of first eophyll petiole; G) detail of the base of an aculeus on the petiole, with sclerified cells; H) transition between adaxial and abaxial sides of eophyll epidermis; I) adaxial face; *J*) abaxial face; K) first eophyll margin, medial region cross-section; L) vascularization and localization of the stomata at the margin 0.1c: first cataphyll, 2c: second cataphyll, ac: aculeus, cc: central cylinder, cor: cortex, col: coleoptyl, ec: expansion cells, end: endodermis, eop: eophyll, ep: epidermis, ex: exodermis, fb: fiber, fs: fiber sheath, lr: lateral root, med: medulla, mx: metaxylem, ps: parenchymal sheath, pe : pericycle, pf: peripheral fiber, ph: phloem, px: protoxylem, rph: raphids, sc: sclerenchyma, sf: subepidermal fiber, st: stomata, vb: vascular bundle, xy: xylem. Scale: A = 1000 μm, B, E, G, I - J, L = 100 μm, C, F = 500 μm, D = 50 μm, H = 150 μm, J = 150 μm, K = 200 μm.

with the seedling axis. This root may be curved, and not entirely visible in longitudinal section (Fig. 6C, I).

At the second cataphyll development stage, the arrangement of these two roots is more or less evident in longitudinal section (Fig. 5G, 7A), and other roots subsequently emerge from the primary one (Fig. 7C).

3.7. Seedling anatomy

Prior to actual emergence, the first eophyll can be identified by its plicate shape, as well as by the differentiation of new leaf primordia at the stem meristem apex (Fig. 5F). Cataphylls are intensely vascularized (Fig. 5D). At this stage, there is no clear petiole or central rib, these becoming visible only after the bifurcation (expansion) of the first eophyll (Fig. 2E). This eophyll is plicate in cross-section view (Fig. 5H), and located inside the second cataphyll, at the top of the aerial part of the plant, showing no evidence of a pinnate shape. In the developed seedling, the coleoptile begins to wither (Fig. 7A), and aculei (spines) project from the cataphyll epidermis and from the first eophyll petiole (Fig. 7B, G - H). Elongated, raphid-containing idioblasts occur in the cataphyll parenchyma (Fig. 7B).

The primary root has a papillary epidermis, an exoderm composed of irregular cells, 6–7 layers of subepidermal fibers, a cortex rich in intercellular spaces, and a central cylinder formed by eight xylematic tubes, surrounded by a pericycle followed by an endoderm with a U-shaped thickening (Fig. 7C - E). Lateral roots arise from the root pericycle, which is already externally differentiated (Fig. 7C). A sclerified central tube lies within the central cylinder (Fig. 7E).

The first eophyll petiole is grooved at the base, adaxially plane and abaxially rounded in the median region, with a sclerified-based aculeus (Fig. 7F - G); internally, marginal and cortical collateral bundles formed by isodiametric cells can be seen. The leaf blade has parallel veins, an uniseriate epidermis, with cells rectangular in longitudinal view. Tetracyclic stomata occur on both faces, but in greater numbers on the abaxial face (Fig. 7H - J). The cuticle is thin, and the epidermis is papillose in the abaxial region, with stomata located just above the other epidermal cells level. Expansion tissue cells underline the epidermis in leaf folds, and a sclerified hypodermis occurs in bundles of subepidermal fibers.

The mesophyll is homogeneous, with chloroplasts visible in the parenchymatous cells close to the adaxial epidermis; extensive subepidermal fibers and fiber bundles lie dispersed within the parenchymatous mesophyll. Vascular bundles are collateral, with xylem facing the upper surface, and abundant perivascular fibers protected by a parenchymatous sheath (Fig. 7K - L). No silica bodies were found in the eophyll.

4. Discussion

The *Astrocaryum acaule* seeds described in this study are usually spherical. Araújo (2005) describes this shape for the seeds of an *A. acaule* population from lowland Amazonian, with a mean size of 12.79 mm, and defines the two superficial depressions as caused by the expansion of the endocarp in the region of the aborted ovules. According to her, when up to three seeds form inside a single fruit, endocarp maturation and hardening compress them, producing the flattened appearance of the seed face adjacent to the locules' septa. Under natural conditions, *A. acaule* seeds are often dispersed with the rigid endocarp intact, affording protection (Araújo, 2005). Morphological and physiological studies of palms (i.e. Ferreira, 1996; Migliaccio, 2002) usually treat the endocarp + seed as a single unit, “the seed”. However, in the current study, the seed endocarp was removed to accelerate germination, an approach already adopted for other studies on *Astrocaryum* species (Elias et al., 2006; Ferreira and Gentil, 2006; Nazário and Ferreira, 2010). According to Ferreira and Gentil (2006), drying facilitates the detachment of the seed from the endocarp, as in *A. aculeatum*. In *Sabal palmetto* (Walt.) Lodd. ex Schultes, the reportedly least destructive method is chemical scarification of intact seeds with sulfuric acid (Dewir et al., 2011). For *Astrocaryum huaimi* Mart., removing the seed coat near the hilum promotes germination with less risk of contamination of the seed interior (Souza et al., 2014).

Another character addressed by removing the endocarp around the seed is dormancy, which is not yet fully understood in palms, but has been the subject of recent studies (Ferreira and Gentil, 2006; Baskin and Baskin, 2013; Meerow and Broschat, 2017). This strategy allows viable embryos to germinate throughout the year, thereby providing resistance to stresses that might otherwise eliminate all individuals of a crop of dispersed seeds at the onset of their development (Fowler and Bianchetti, 2000). According to Guimarães et al. (2000), variation in seedling emergence distribution in time and space may be associated with temperature variation in the natural environment. In *Tridax procumbens* L. (Asteraceae), the authors found germination to be staggered in nature, but uniform under laboratory conditions. According to Dorneles (2010), dispersion of germination over time greatly enhances species establishment and facilitates restoration in fragmented environments, but may hamper management activities when native species with this dormancy pattern are sown together with others of economic importance that do not present dormancy (Souza et al., 2015).

The embryonic axis of *A. acaule* is located proximally, and obliquely oriented. Araújo (2005) describes the *A. acaule* embryo as cylindrical, straight, and lacking constrictions between the proximal and distal regions. The embryo shape observed in the current study does not support Tomlinson's (1990) observation that, in palms with adjacent development, the embryo is curved, with an oblique embryonic axis. The characters observed here for *A. acaule* indicate that this concept cannot be universally applied in species belonging to families with adjacent germination, and may be more similar to *Elaeis* (Rees, 1960), where the embryo is straight and has a persistent radicle. The reduced stem of *A. acaule* can curve while the seedling axis is elongating. The embryonic curvature and the oblique nature of the embryonic axis facilitate development after germinative bud emergence, and in species with adjacent development the cotyledonary sheath region and stem primordia can take on a curved shape, as in the case of the "saxophone stem" of *A. aculeata* (Nascimento e Souza et al., 2017).

Aguiar and Mendonça (2001); Gentil and Ferreira (2005), and Luz et al. (2012) describe the first emergent structure as the cotyledonary petiole. However, because this region is the one protecting the embryonic axis, it does, in fact, correspond to the cotyledonary sheath. In the current study, the term “germinative bud” was adopted because it is more comprehensive, and has been already used for this structure by Queiroz and Bianco (2009) when describing the germination of *Oenocarpus bacaba* Mart., a species of tribe Cocoseae. The vertical extension of the cotyledonary sheath forms the coleoptile, which longitudinally orients the leaf primordia during shoot development (Tomlinson, 1990). According to Tillich (2007), the coleoptile is often confused with a ligule, which concept should be restricted to a structure that lies on the adaxial surface of bifacial leaves, whereas coleoptile is a tubular structure produced by meristematic activity in the marginal tissues of the cotyledonary sheath connected to a unifacial hyperphyll. The germinative bud shape resembles that described by Araújo (2005) for *A. acaule*, except for the constriction observed in the median region, which corresponds to the apocole located proximally between the differentiating haustorium and the cotyledonary sheath. The same author also reports the lack of evidence of a cotyledonary cleft in the embryo. Although the cotyledon is analogous to a first embryonic leaf, in the Arecaceae it does not have a bifacial aspect, which Tillich (2007) used as an argument for the use of a different nomenclature for the structure, as well as proposing the term “hyperphyll” for the area separated from the distal region (haustorium + apocole). Henderson (2006) does not include the haustorium in the hyperphyll region, restricting the concept to the elongation zone (apocole). Regarding the delay in the protrusion of the primary root, Aguiar and Mendonça (2001) report the radicular

pole emergence before the appearance of cataphylls in *E. precatoria*.

Gentil and Ferreira (2005) give 99 and 253 days as the mean time for bud formation, and expansion of the first eophyll, respectively, in *A. aculeatum*. According to Meerow (2004), a widespread capacity for dormancy in palms means that an estimated 25% of species studied in the family take more than 100 days to germinate, and have a germination success rate below 20%. In *Archontophoenix cunninghamii* H. Wendl. & Drude, the germinative bud can be observed within 9 and 45 days (Luz et al., 2012).

In the current study, we described whitish cataphylls, as well as the possibility that root emission could be delayed. In *Euterpe precatoria* Mart., Aguiar and Mendonça (2001) describe the production of morphologically similar, purple-colored cataphylls. In *Euterpe edulis* Mart., the primary root is already elongating when the first cataphyll emerges (Accorsi and Barros, 1974), as later described also for *Astrocaryum aculeatum* Mart. (Gentil and Ferreira, 2005). Neto et al. (2010) reported accumulation of reserves and abundant vascular traces between the insertion of the root and the cataphylls along the seedling development for *Euterpe oleracea* Mart.

The first eophyll is bifid and plicate. Aguiar and Mendonça (2001) describe evidence of a pinnate form in the first eophyll of *E. precatoria* prior to its emergence. The haustorium growth occurs as a result of endosperm reserve consumption, and is evident throughout the seedling development. In *Elaeis guineensis* Jacq., the haustorium epidermis secretes enzymes that digest endosperm lipids, thus actively participating in the mobilization of reserves to the growing seedling (Opute, 1975). This may suggest that further studies are required to establish the moment at which seedlings of this species become independent of seed reserves. In *E. oleracea*, the haustorium has consumed most of the seed volume by the 100$^{th.}$ day, the approximate time when the first eophyll emerges (Neto et al., 2010).

The first emerged oblique root was described herein as a “lateral root”. Tomlinson (1990) and other authors, earlier and later (Rees, 1960; Accorsi and Barros, 1974; Gentil and Ferreira, 2005; Oliveira et al., 2010), have defined this as the primary root. The root cap described in this study was described as a coleorhiza for seedlings of *E. edulis* (Accorsi and Barros, 1974). We term it a root cap due to the absence of a protective, coleorhiza-like, sheath in the previous stages of radicle development, as recorded also in other monocotyledons (Tillich, 2007). The occurrence of raphids near the *A. acaule* radicle was common at this stage, although Araújo (2005) does not mention raphids in the embryonic axis of the species at the embryo stage. Tomlinson (1990) further notes that, as result of the curvature of both embryo and embryonic axis, this root, which emerges as a thin and oblique structure, is soon replaced by an adventitious root. This root is defined in the current study as the true primary root. Tomlinson also states that this first narrow and angular root is characteristic of palms with adjacent germination, and that this character is typical of subfamily Arecoideae. However, due to its origin in the peripheral region of the initial area of the radicle, this structure was classified as the first lateral root in this study. For *Livistona rotundifolia* (Lam.) Mart., a palm of subfamily Coryphoideae with remote initial growth, Viana et al. (2016) considered that the lateral roots began to develop from the interior of the vascular cylinder, even while the cotyledonary sheath was still undergoing differentiation.

The structure defined as the “primary root” in the current study has been termed the first adventitious root in other studies (Tomlinson, 1990; Gentil and Ferreira, 2005), probably because of the oblique nature of the embryonic axis within the cotyledonary sheath. However, one must consider the continuity of root tissues with the meristematic tissues of the hypocotyl region (Figs. 5G, 7 A), even though it is not the first root to emerge from the cotyledonary sheath. This situation underscores the need for anatomical investigation of this zone in germination studies of adjacent germinating palms, specifically, to avoid misunderstandings and classification confusion arising from observations based primarily on external morphology. Henderson (2006) considers the root protrusion angle as a key characteristic for the classification of palm seedling germination types, and cites the example of *Astrocaryum alatum* Loomis. However, in this study, this angle was variable and not diagnostic. In *E. precatoria*, a large number of lateral roots have already emerged by the time the first cataphyll appears, originating from the pericycle of the primary root (Aguiar and Mendonça, 2001). Henderson (2006) describes the occurrence of abundant adventitious roots in *A. alatum*. Root system formation is a complex process that has been little discussed in the palm development literature. Established standards do not apply to all members of the family, and knowledge of this topic is often lacking for tropical species (Tomlinson, 1990, 2006).

In *E. precatoria*, up to three new leaf primordia can be observed simultaneously (Aguiar and Mendonça, 2001). At the *A. aculeatum* first eophyll stage, the coleoptile is still expanding (Gentil and Ferreira, 2005). The seedling root features are similar to those described for *Oenocarpus minor* Mart. by Oliveira et al. (2010), and are common characters in monocotyledons (Esau, 1976). Palm literature commonly refer the pointed emergences usually found in various parts of the plant as “spines” (Henderson, 1995; Tomlinson, 1990, 2006; Stauffer, 2000). As vascular traces were not found in the structures observed on the surface of cataphylls and eophylls, we termed these “aculei”, following recent studies on palms (Batagin-Piotto et al., 2012) and an established anatomical concept (Dutta, 2000; Simpson, 2010; Judd et al., 2009). The leaf expansion tissue described in this study confers the ability to expand as the leaf matures, or according to the water resources available to the plant (Tomlinson, 1990). Paula (1975) describes a hypodermis in *E. oleracea*, and Tomlinson (1990) states that its commonness in the Arecaceae. In the leaves of *Mauritia flexuosa* L. f., at various stages of plant development, Passos and Mendonça (2006) report the presence of silica bodies accompanying the fibers, and distributed in the epidermal cells, but not a hypodermis.

5. Conclusions

Astrocaryum acaule is a species with adjacent germination, featuring a coleoptile formed from the cotyledonary sheath, and variable germination time. Its maintenance in the natural environment and independence of nutritional reserves deserves further investigation. Anatomical characteristics reported in this study increase the knowledge of Amazonian palms and the organogenesis of their initial growth stages, and clarify uncertainties concerning characters not previously covered in the literature. Studies of palms with other initial growth patterns are needed, as is the use of anatomical tools in such studies. The current study provides a detailed morphological analysis of growth stages that may differ between the genus *Astrocaryum* and other palms, such as the characteristic formation of the root system. The results presented in our study enhance our knowledge of the Amazonian flora natural history, enabling future studies and assisting conservation.

Acknowledgements

We are indebted to the Comissão de Aprimoramento de Pessoal de Nível Superior (CAPES) for the study grant, to the team at the Laboratório de Botânica Agroflorestal (LABAF) for infrastructural help, to Manoel Roberto Pereira Viana for instruction and technical help, to Dr. Adrian Barnett and Pedro Manuel dos Santos with the English text.

References

Accorsi, W.R., Barros, M.A.A., 1974. Morfologia do fruto e da semente de *Euterpe edulis* Mart. An. Esc. Super. Agric. Luiz de Queiroz 31, 701–711.

Aguiar, M.O., Mendonça, M.S., 2001. Aspectos morfológicos da germinação e do desenvolvimento plantular em *Euterpe precatoria* Mart. (açaí-do-Amazonas). Acta Amaz. 31 (4), 687–691.

Araújo, M.G.P., 2005. Morfo-anatomia e desenvolvimento dos frutos e sementes de três espécies da subfamília Arecoideae (Arecaceae). Doctoral thesis. INPA, Manaus, AM.

Baskin, J.M., Baskin, C.C., 2013. What kind of seed dormancy might palms have? Seed Sci. Res. 24, 17–22. https://doi.org/10.1017/S0960258513000342.
Batagin-Piotto, K.D., Almeida, C.V., Piotto, F.A., Almeida, M., 2012. Anatomical analysis of peach palm (*Bactris gasipaes*) leaves cultivated in vitro, ex vitro and in vivo. Braz. J. Bot. 35 (1), 71–78.
Bukatsch, F., 1972. Bemerkungen zur Doppelfärbung Astrablau-Safranin. Mikrokosmos 61 (8), 255.
Cintra, R., Ximenes, A.C., Gondim, F.R., Kropf, M.S., 2005. Forest spatial heterogeneity and palm richness, abundance and community composition in Terra Firme forest, Central Amazon. Rev. Bras. Bot. 28 (1), 75–84.
Dewir, Y.H., El-Mahrouk, M.E.S., Naidoo, Y., 2011. Effects of some mechanical and chemical treatments on seed germination of *Sabal palmetto* and *Thrinax morrisii* palms. Asian J. Res. Crop Sci. 5 (3), 248–253.
Dorneles, M.C., 2010. Padrões de germinação dos diásporos e emergência das plântulas de espécies arbóreas do cerrado, do Vale do Rio Araguari. MG. Master's thesis. Universidade Federal de Uberlândia, Instituto de Biologia, Uberlândia, MG.
Dransfield, J., Uhl, N.W., Asmussen, C.B., Baker, W.J., Harley, M.M., Lewis, C.E., 2008. Genera Palmarum: The Evolution and Classification of Palms. Kew Publishing, Kew.
Dutta, A.C., 2000. A Class-book of Botany. Oxford University Press, Oxford.
Elias, M.E.A., Ferreira, S.A.N., Gentil, D.F.O., 2006. Emergência de plântulas de tucumã (*Astrocaryum aculeatum*) em função da posição de semeadura. Acta Amaz. 36 (3), 385–388. https://doi.org/10.1590/S0044-59672006000300016.
Esau, K., 1976. Anatomy of Seed Plants, 3rd. edn. John Willey and Sons, New York.
Ferreira, S.A.N., 1996. Maturação fisiológica de sementes de pupunheira (*Bactris gasipaes* Kunth). Doctoral thesis. PPGBTRN/INPA/UFAM, Manaus, AM.
Ferreira, S.A.N., Gentil, D.F.O., 2006. Extração, embebição e germinação de sementes de tucumã (*Astrocaryum aculeatum*). Acta Amaz. 36 (2), 141–146.
Fowler, A.J.P., Bianchetti, A., 2000. Dormência em sementes florestais. Embrapa Florestas, Colombo, pp. 27.
Franklin, G.L., 1945. Preparation of the thin sections of synthetic resins and wood-resin composites, and a new macerating method for wood. Nature 155, 51.
Gentil, D.F.B., Ferreira, S.A.N., 2005. Morfologia da plântula em desenvolvimento de *Astrocaryum aculeatum* Meyer (Arecaceae). Acta Amaz. 35 (3), 337–342.
Groth, D., Liberal, O.H.T., 1988. Catálogo de identificação de sementes. Fundação Cargill, Campinas. pp. 182.
Guimarães, S.C., Souza, I.F., Pinho, E.V.R.V., 2000. Efeito de temperaturas sobre a germinação de sementes de erva-de-touro (*Tridax procumbens*). Planta Daninha 18 (3), 457–464.
Gurski, C., 2007. Estudos comparativos de plântulas e plantas jovens de duas espécies de *Ormosia* Jackson provenientes de ambientes distintos - restinga e mata ciliar. Master's thesis. Universidade Federal de Mato Grosso do Sul, Mato Grosso do Sul.
Henderson, A., 1995. The Palms of the Amazon. Oxford University Press, New York.
Judd, W.S., Campbell, C.S., Kellogg, E.A., Stevens, P.F., Donoghue, M.J., 2009. Sistemática Vegetal - Um Enfoque Filogenético. Artmed Editora.
Kraus, J.E., Arduin, M., 1997. Manual básico de métodos em morfologia vegetal. Edur, Seropédica, RJ, pp. 198.
Lorenzi, H., 2010. Flora brasileira: Arecaceae (palmeiras). Plantarum, Nova Odessa, pp. 384.
Luz, P.B., Pivetta, K.F.L., Neves, L.G., Sobrinho, S.P., Barelli, M.A.P., 2012. Caracterização morfológica do diásporo e da plântula de *Archontophoenix cunninghamii* (Arecaceae). Comun. Sci. 3 (4), 244–248.
Meerow, A.W., 2004. Palm Seed Germination. University of Florida, IFAS Extension, Fort Lauderdale(Bulletin, 274). http://edis.ifas.ufl.edu/pdffiles/EP/EP23800.pdf. Access in 25/04/2018.
Meerow, A.W., Broschat, T.K., 2017. Palm Seed Germination. University of Florida cooperative Extension Service, Institute of Food and Agricultural Sciences. EDIS Access in 25/04/2018. http://edis.ifas.ufl.edu/ep238.
Migliaccio, C., 2002. Germinating Gastrococos – Quickly and Easily. Palms 46 (2) Access in 20/11/2018. http://www.palms.org/palmsjournal/2002/gastrococos.htm.
Mourão, K.S.M., Dias-Pinto, D., Souza, L.A., Moscheta, I.S., 2002. Morfo-anatomia da plântula e do tirodendro de*Trichilia catigua* A. Juss., *T. elegans* A. Juss. e *T. pallida* Sw. (Meliaceae). Acta Sci. 24 (2), 601–610.
Nascimento e Souza, J., Ribeiro, L.M., Mercadante-Simões, M.O., 2017. Ontogenesis and functions of saxophone stem in *Acrocomia aculeata* (Arecaceae). Ann. Bot. 119, 353–365.
Nazário, P., Ferreira, S.A.N., 2010. Emergência de plântulas de*Astrocaryum aculeatum* G. May. em função da temperatura e do período de embebição das sementes. Acta Amaz. 40 (1), 165–170. https://doi.org/10.1590/S0044-59672010000100021.
Neto, M.A.M., Lobato, A.K.S., Alves, J.D., Goulart, P.F.P., Laughinghouse, H.D., 2010. Seed and seedling anatomy in *Euterpe oleracea* Mart. During the germination process. J. Food Agric. Environ 8, 1147–1152.
O'Brien, T.P., Feder, N., McCully, M.E., 1964. Polychromatic staining of plant cell walls by toluidine blue O. Protoplasma 59, 368–373.
Oliveira, A.B., Mendonça, M.S., Araújo, M.G.P., 2010. Aspectos anatômicos do embrião e desenvolvimento inicial de *Oenocarpus minor* Mart.: uma palmeira da Amazônia. Acta Bot. Bras. 24 (1), 20–24.
Opute, F.I., 1975. Lipid composition and the role of the haustorium in the young seedling of the West African oil palm, *Elaeis guineensis* Jacq. Ann. Bot. 39 (5), 1057–1061.
Passos, M.A.B., Mendonça, M.S., 2006. Epiderme dos segmentos foliares de*Mauritia flexuosa* L. f. (Arecaceae) em três fases de desenvolvimento. Acta Amaz. 36 (4), 431–436.
Paula, J.E.D., 1975. Anatomia de*Euterpe oleracea* Mart. (Palmae da Amazônia). Acta Amaz. 5 (3), 265–278.
Queiroz, M.H., 1986. Botão germinativo do palmiteiro como indicador da germinação. Rev. Bras. Sementes 2 (1), 55–59.
Queiroz, M.S.M., Bianco, R., 2009. Morfologia e desenvolvimento germinativo de *Oenocarpus bacaba* Mart. (Arecaceae) da Amazônia Ocidental. Rev. Árvore 33 (6), 1037–1042.
Rees, A.R., 1960. Early development of the oil palm seedlings. Principes 4, 148–150.
Rojas-Robles, R., Stiles, F.G., 2009. Analysis of a supra-annual cycle: reproductive phenology of the palm *Oenocarpus bataua* in a forest of the Colombian Andes. J. Trop. Ecol. 25, 41–51.
Santos-Silva, E.N., 2008. *Biotupé:* Meio Físico, Diversidade Biológica E Sociocultural Do Baixo Rio Negro, Amazônia Central, vol. 2 UEA Edições, Manaus.
Simpson, M.G., 2010. Plant Systematics. Academic press.
Souza, A.L., Sales, J.F., Campos, R.C., Neto, A.R., Silva, F.G., 2014. Superação da dormência de sementes de Tucum (*Astrocaryum huaimi* Mart.). Semina: Ciênc. Agrár. 35 (2), 749–758.
Souza, G.C., Timossi, P.C., Netto, A.P.C., Rodrigus, M.J., Alcir, L., Filho, F., 2015. Germinação de sementes de mucuna-preta submetidas a diferentes períodos de armazenamento. Rev. Bras. Energy Renov. 4, 72–83.
Stauffer, F.W. (Ed.), 2000. Contribución al estudio de las palmas (Arecaceae) del Estado Amazonas, Venezuela, vol. 10. Sci. Guaianae, pp. 1–197.
Tillich, H.J., 2007. Seedling Diversity and the Homologies of Seedling Organs in the Order Poales (Monocotyledons). Ann. Bot. 100, 1413–1429.
Tomlinson, P.B., 1990. The Structural Biology of Palms. Oxford University Press, New York, pp. 477.
Tomlinson, P.B., 2006. The uniqueness of palms. Bot. J. Linn. Soc. 151, 5–14.
Uhl, N.W., Dransfield, J., 1987. Genera Palmarum. A Classification of Palms Based on the Work of Harold E. Moore-jr. Allen Press, Lawrence, Kansas, pp. 610.
Viana, F.A.P., Costa, A.P., Moro, F.V., Pivetta, K.F.L., 2016. Morpho-anatomical characterization of diaspores and seedlings of *Livistona rotundifolia*. Ornam. hortic. 22 (3), 249–255. https://doi.org/10.14295/oh.v22i3.924.